Journal of Inorganic and General Chemistry
ZAAC
Zeitschrift für anorganische und allgemeine Chemie
www.zaac.wiley-vch.de
RESEARCH ARTICLE

DOI: 10.1002/zaac.202100358

Li_3As and Li_3P revisited: DFT modelling on phase stability and ion conductivity

Florian Wegner,[a] Franziska Kamm,[a] Florian Pielnhofer,[a] and Arno Pfitzner*[a]

Dedicated to Prof. Josef Breu on the occasion of his 60th birthday.

Phase pure Li_3As and Li_3P were synthesized from the elements by a high temperature route. Crystal structures were refined from powder X-ray diffraction data. The title compounds were further characterized by difference thermal analysis, temperature dependent X-ray powder diffraction and impedance spectroscopy, proving unexpected Li ion conductivity for Li_3As. High pressure behaviour of the title compounds was modeled via density functional theory, confirming the experimentally reported cubic modifications of Li_3P and Li_3As.

Introduction

Compared to Li_3N, less information on the heavier homologues Li_3P and Li_3As can be found in literature concerning structures and physical properties.[1,2,3] α-Li_3N (space group *P6/mmc*, no. 191) transforms to β-Li_3N (*P6$_3$/mmc*, no. 194) at a pressure of about 0.5 GPa, the β-modification of Li_3N is isotypic to the Li_3P and Li_3As ambient temperature modifications, adopting the [Na_3As]-type structure (structure types are written in square brackets throughout the manuscript). Li_3N undergoes a further phase transition at 40 GPa to the cubic [Li_3Bi]-type structure (γ-Li_3N, *Fm*$\bar{3}$*m*, no. 225).[1] In 2003, the phase transition of hexagonal Li_3P to the [Li_3Bi]-type structure was reported.[2] Investigations of Li_3As under high-pressure are quite rare, only in 1991 a transformation to a high-pressure modification was mentioned.[3] The cubic [Li_3Bi]-type structure exists for all Li_3Pn compounds with *Pn* = N, P, As, Sb and Bi. Again, numerous data is available about the ionic conductivity of Li_3N and some ternary or even quaternary nitrides.[4,5,6,7] Li_3N was discovered to be a good ion conductor quite early, conductivity measurements on polycrystalline samples (1976) and single crystals (1977) can be found in literature.[4,5] Conductivity properties of Li_3P and Li_3As were reported in 1994.[8] The data indicate metallic behaviour of Li_3As instead of ionic conductivity as shown for Li_3N and Li_3P in the same publication. Calculated band gaps of Li_3N (1.14 eV), Li_3P (0.72 eV) and Li_3As (0.65 eV) can be found in the literature and contradict the drastic change from the ion conducting phosphide to a metallic character as proposed for Li_3As.[9] In the last decade, phosphidosilicates became an interesting group of compounds in terms of ion conductivity.[10,11,12,13] More and more complex structures and their different ion conductivities were studied. In 2020 Li_2SiAs_2, a new ternary arsenide showing lithium-ion conductivity was reported.[14] The ionic conductivity of Li_2SiAs_2 is significantly higher than for the well characterized lighter homologues Li_2SiP_2 and Li_2SiN_2.[15,16] We synthesized Li_3P and Li_3As from the elements and investigated the samples by thermal analysis, temperature dependent X-ray powder diffraction (XRPD) experiments, impedance spectroscopy and density functional theory (DFT) modeling.

Results and Discussion

Li_3P and Li_3As were synthesized by heating the elements in a graphite crucible encapsulated in quartz tubes to elevated temperatures. The obtained beige (Li_3P) and brown-red (Li_3As) products can easily be ground and are highly sensitive to moisture. In Figure 1 the refined powder diffraction patterns (Cu–Kα_1 radiation) are displayed. The structure models proposed by Juza were used as starting models for Rietveld refinements.[17] Besides about 1 % traces of Li_2O in Li_3P there are no impurities present in the samples as can easily be judged from the perfect match of measured and calculated diffraction patterns. Li_3As and Li_3P crystallize in the hexagonal space group *P6$_3$/mmc* with $a = 4.378(1)$ Å, $c = 7.799(1)$ Å, $V = 129.5(1)$ Å^3 and $Z = 2$ for Li_3As and $a = 4.254(1)$ Å, $c = 7.584(1)$ Å, $V = 118.9(1)$ Å^3 and $Z = 2$ for Li_3P. Refinement data are given in Table 1. Wyckoff positions, atomic coordinates and displacement parameters are given in Table 2. The compounds can be described to adopt the [Na_3As]-type structure. It has to be mentioned that Na_3As itself crystallizes in the [Cu_3P]-type structure.[18] The diffraction patterns of Li_3P and Li_3As do not show any superstructure reflections indicating a similar behaviour as reported for Na_3As and Na_3P recently.[19] The structure of Li_3Pn (*Pn* = P, As) can be

[a] F. Wegner, F. Kamm, Dr. F. Pielnhofer, Prof. Dr. A. Pfitzner
Institut für Anorganische Chemie
Universität Regensburg
Universitätsstraße 31, 93053 Regensburg (Germany)
E-mail: arno.pfitzner@chemie.uni-regensburg.de

Supporting information for this article is available on the WWW under https://doi.org/10.1002/zaac.202100358

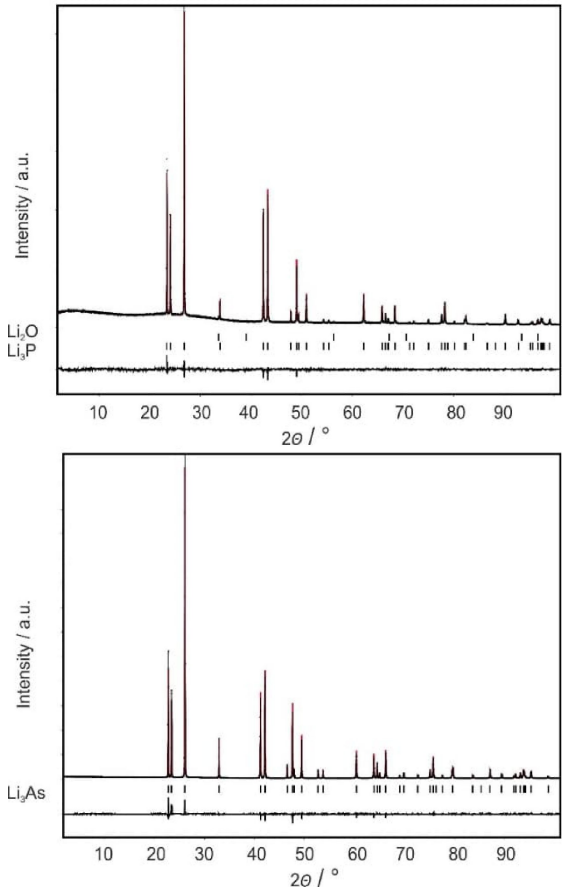

Figure 1. Refined powder diffraction patterns (measured and calculated) of Li_3P (top) and Li_3As (bottom) with difference plot using Cu–Kα_1-radiation at room temperature.

Table 1. Refinement parameters of Li_3P and Li_3As from Rietveld refinement at 20 °C.

Empirical formula	Li_3P	Li_3As
Formula weight/g mol	51.8	95.7
T/K	293	
Radiation wavelength	λ = 1.5406 Å	
Colour	beige	brown-red
Crystal system	Hexagonal	
Space group	*P6₃/mmc*	
a = *b*/Å	4.254(1)	4.378(1)
c/Å	7.584(1)	7.799(1)
V/Å^3	118.9(1)	129.5(1)
Z	2	2
ρ (calc.)/g cm^3	1.45	2.46
Θ range/deg.	$2.00 < 2\,\Theta < 100.985$	
R_p	0.0388	0.0617
R_{wp}	0.0486	0.0778
R_{exp}	0.0378	0.0449
GOOF	1.28	1.73

described as a layered structure, consisting of graphite-like six-membered rings of Li*Pn* in *a*–*b* direction with a second Li-layer separating the sheets in *c* direction as displayed in Figure 2. The

Table 2. Wyckoff positions, atomic coordinates and displacement parameters of Li_3P and Li_3As from Rietveld refinement at 20 °C.

Li_3P	Wyckoff position	*x*	*y*	*z*	U_{iso}
Li1	*2b*	0	0	1/4	0.0335(1)
Li2	*4f*	1/3	2/3	0.5843(3)	0.0316(8)
P	*2c*	1/3	2/3	1/4	0.0181(1)
Li_3As					
Li1	*2b*	0	0	1/4	0.051(1)
Li2	*4f*	1/3	2/3	0.5829(6)	0.052(2)
As	*2c*	1/3	2/3	1/4	0.0248(1)

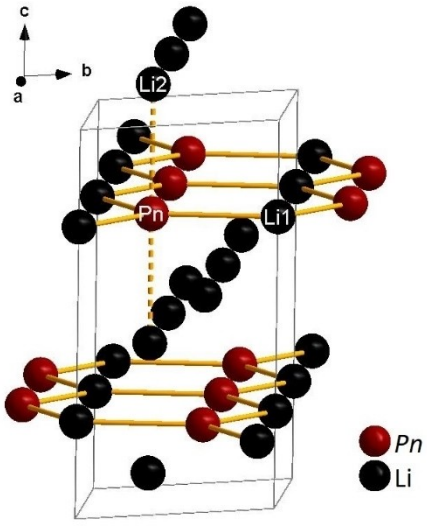

Figure 2. The [Na_3As]-type structure (*P6₃/mmc*, no. 194). Section of the crystal structure of Li_3Pn with Li*Pn* sheets built from Li1 and *Pn* as main structural motive. Li*Pn* sheets are separated by atom layer Li2.

[Li_3Pn_3] rings are built up from Li1 and *Pn*1, the interatomic distances are *d*(Li1-P1) = 2.456 Å and *d*(Li1-As1) = 2.528 Å. The *Pn* atoms in a ring are coordinated by three Li atoms in the layer and two apical Li atoms to form a trigonal bipyramid. The bipyramid is lightly stretched in *c* direction due to longer bond distances in apical direction *d*(Li2-P1) = 2.535 Å and *d*(Li2-As1) = 2.596 Å. The structure is identical to the [β-Li_3N]-type structure, which is known to be a good lithium-ion conductor. A high content of possibly mobile ions in a layered structure gives many clues for potential conduction pathways.

As mentioned above, β-Li_3N undergoes a phase transition from the hexagonal [Na_3As]-type structure to the cubic [Li_3Bi]-type structure at 40 GPa (γ-Li_3N modification). For Li_3P, an analogous phase transition is observed. In 2003 an experiment showed, that hexagonal Li_3P transforms to the cubic modification at 700 °C under a pressure of 4 GPa.[2] Figure 3 displays the cubic [Li_3Bi]-type structure as known for γ-Li_3N, cubic Li_3P, Li_3Sb and Li_3Bi. We modeled the two modifications of Li_3P with DFT calculations for a better understanding of this behaviour of the title compounds. The modelling was extended to Li_3As. For Li_3As, a high-pressure modification was mentioned in literature,

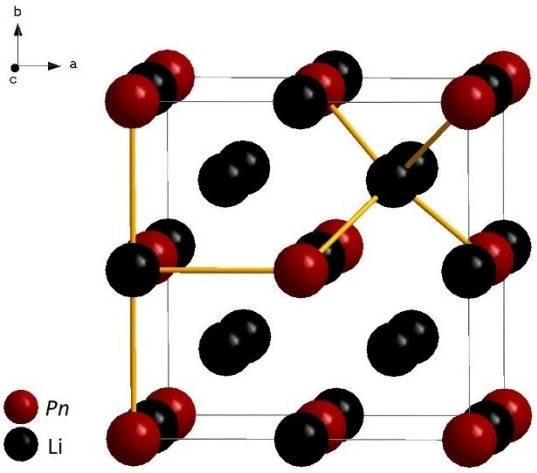

Figure 3. Unit cell of the [Li_3Bi] structure ($Fm\bar{3}m$, no. 225) type as it is known for γ-Li_3N, cubic Li_3P, Li_3Sb and Li_3Bi. Lithium atoms occupy all tetrahedral and octahedral voids of the ccp arrangement of *Pn*-atoms.

providing not that much information compared to Li_3N or Li_3P. In Figure 4 a *E*-*V*-plot for different modifications of Li_3P is displayed. The calculations show that the hexagonal modification is about 3.7 kJ mol^{-1} more stable than the cubic one at ambient pressure. For lower cell volumes the cubic modification shows higher stability. Analogously, *E*-*V*-curves for Li_3As were calculated. In this case, the hexagonal modification is about 6.5 kJ mol^{-1} more stable than the cubic one. We find a transition pressure of 1.1 GPa for the transition from hexagonal Li_3P to the cubic modification by fitting the data for both compounds to a Birch-Murnaghan equation of state (EoS) and subsequently calculate the enthalpy vs pressure diagrams (see SI, Figs. S6 and S7). From experiments a higher value of about 4 GPa was derived, but this value is not directly comparable to modelled properties as it comes not from in-situ data, but from a measurement at ambient conditions on a sample that was prepared under pressure before. For Li_3As we calculated a transition pressure of 1.5 GPa, i.e., a slightly higher pressure than for Li_3P. Anyhow, it is still in the same range as for Li_3P and comparable to the value of 4.5 GPa given in the literature.[3] We therefore can state that the high-pressure modification of Li_3As crystallizes in the cubic [Li_3Bi]-type structure as reported earlier. The transition pressures for Li_3P and Li_3As are very similar, indicating comparable physical properties.

For all binary pnictides Li_3Pn with *Pn* = N, P, As, Sb, and Bi a cubic [Li_3Bi]-type modification exists. For *Pn* = N, P, and As pressure is necessary to transform the compounds to the higher symmetric modification, whereas Li_3Sb can be prepared in both modifications by just varying the temperature used for synthesis.[2] Applying temperatures >650 °C leads to the formation of cubic Li_3Sb, lower temperatures result in the hexagonal [Na_3As]-type modification. The parameters for the transformation of the low symmetry structure to the higher symmetric one are summarized in Table 3. Temperature dependent powder diffraction data in the same temperature range as for impedance spectroscopy were recorded to monitor unit cell expansion. Li_3Pn (*Pn* = P, As) samples show no phase transition in the temperature range from room temperature to

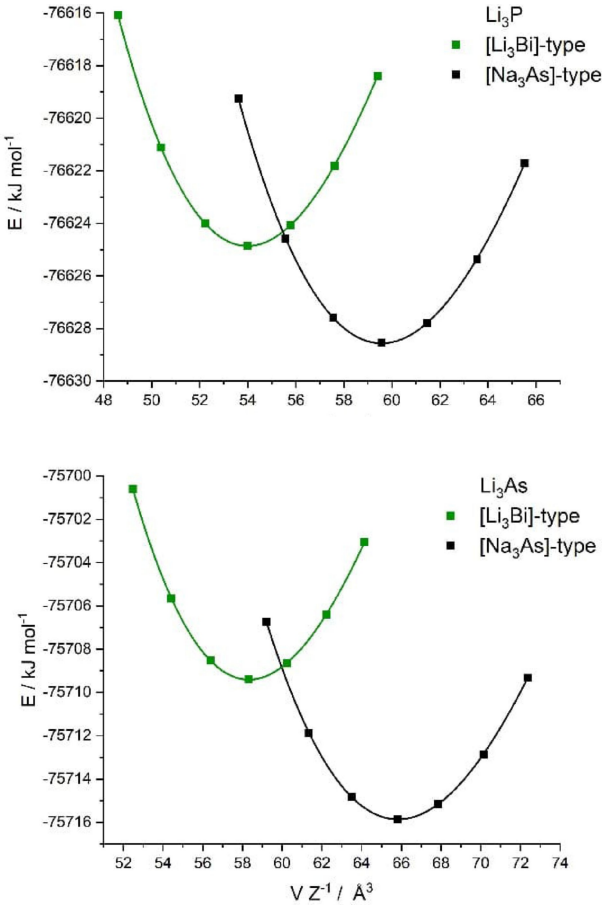

Figure 4. Energy vs. volume curves of Li_3P (top) and Li_3As (bottom). The [Na_3As]-type structure is stable at ambient conditions for both compounds. Applying pressure should lead to a phase transition to the cubic [Li_3Bi]-type structure, which is more stable at lower volumes.

Table 3. Parameters for the transformation from [Na_3As]-type structures to [Li_3Bi]-type structures in Li_3Pn-materials (Pn=N, P, As, Sb, Bi). While the transformation of Li_3N, Li_3P and Li_3As is pressure-induced, Li3Sb already transforms at higher temperatures and Li_3Bi is stable at ambient conditions due to increasing metallic character of the heavier homologues.

Transformation of Na_3As – like Li_3Pn to Li_3Bi – like modification	Driving force	Experimental parameters (calculated, this work)
Li_3N	Pressure	40 GPa[1]
Li_3P	Pressure & Temperature	4 GPa; 700 °C [2] (1 GPa)
Li_3As	Pressure	4.5 GPa [3] (1.5 GPa)
Li_3Sb	Temperature	T > 650 °C[2]
Li_3Bi	Ambient conditions	

300 °C what is consistent with the calculated properties. The cell parameters *a*, *c* and *V* rise linearly with increasing temperature. High-temperature XRPD data are given in the supporting information (Tables S1, S2; Figures S3, S4).

The Li-migration pathways in α- and β-Li_3N are already known from DFT modelling and also conductivity measurements on single crystals of α-Li_3N.[5] In β-Li_3N, which is isotypic to Li_3P and Li_3As, the ion conductivity mainly arises from Li2 moving between the Li*Pn*-layers built up from Li1 and *Pn*.[20] Similar conductivity properties are expected for Li_3P and Li_3As due to their structural similarity. Impedance spectroscopic measurements on cold pressed pellets of Li_3P and Li_3As show a semicircle for high frequencies and a low frequency arc in Nyquist plots (see Figure 5). Specific conductivities were extracted from complex Nyquist plots followed by subsequent correction of geometrical parameters and experimental density of the pellets (89% (Li_3P) and 94% (Li_3As) compared to crystallographic data). For Li_3P conductivities of σ_{spec} (50 °C) = $3.0(6)\cdot10^{-8}$ S·cm^{-1} to of σ_{spec} (300 °C) = $1.1(1)\cdot10^{-4}$ S·cm^{-1} were extracted, an activation energy of 0.53(1) eV was determined. For Li_3As conductivities of σ_{spec} (50 °C) = $1.5(3)\cdot10^{-7}$ S·cm^{-1} to of σ_{spec} (300 °C) = $4.5(4)\cdot10^{-4}$ S·cm^{-1} and an activation energy of 0.50(1) eV were extracted. Conductivity data is summarized in Table 4. The Arrhenius plot (see Figure 6) clearly shows the higher conductivity of Li_3As as compared to Li_3P. The possibly higher mobility of lithium in the framework of Li_3As can be explained by the better polarizability of the As^{3-} anion compared to P^{3-} in Li_3P. As already mentioned, even the ternary compounds Li_2SiAs_2 and Li_2SiP_2 match the trend, that arsenides have higher conductivities than phosphide-based isostructural materials. Again, the higher polarizability of the arsenide anion can be regarded as one reason for this observation. Our investigation clearly demonstrates that Li_3As has a conductivity behaviour that is similar to Li_3N and Li_3P. This is in perfect accord with the brown-red colour of the brittle samples. Earlier publications classifying Li_3As as a metal only mentioned the decreasing ionicity from Li_3N to Li_3As. However, this contradicts the calculated band gap of 0.65 eV for Li_3As, which clearly opposes a metallic behaviour. The capacities extracted from the fits of the Nyquist plots are in the typical range of Li ion conductors. However, a small electronic contribution to the total conductivity of Li_3As and Li_3P cannot be ruled out from the available measurements. Measurements on single crystalline samples as known for α-Li_3N would be interesting to further verify the different contributions to the conductivities under discussion.[5] Growth of single crystals of Li_3P and Li_3As remains challenging due to toxicity and reactivity of these compounds. Our conductivity measurements do not match previous data.[8] This might be explained by differences in the experimental setups. Literature reported conductivities were determined by d–c measurements instead of a–c impedance measurements which might explain the severe discrepancies. In addition, Li_3P and Li_3As are highly sensitive to moisture and are extremely corrosive at elevated temperatures. Therefore, we performed all measurements in an Ar filled glovebox.

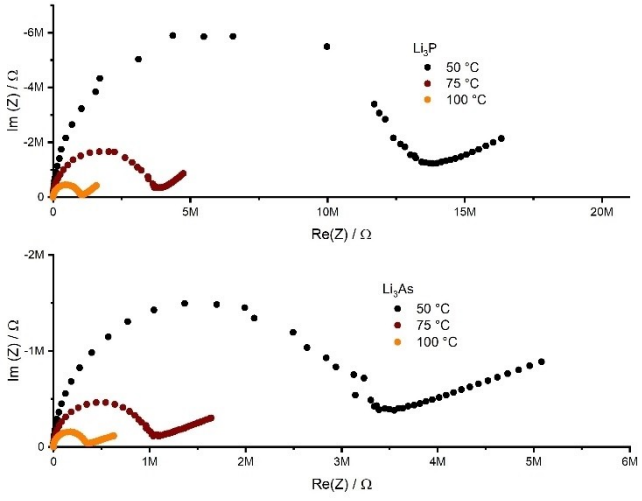

Figure 5. Nyquist plots of Li_3P (top) and Li_3As (bottom) from impedance measurements showing a semicircle (high frequencies) and a tail (low frequencies).

Table 4. Conductivity data of Li_3P and Li_3As from impedance spectroscopy.

	Li_3P	Li_3As
σ_{spec} (50 °C)/S·cm^{-1}	$3.0(6)\cdot10^{-8}$	$1.5(3)\cdot10^{-7}$
σ_{spec} (100 °C)/S · cm^{-1}	$4.3(4)\cdot10^{-7}$	$1.6(4)\cdot10^{-6}$
σ_{spec} (150 °C)/S · cm^{-1}	$3.2(2)\cdot10^{-6}$	$9.4(1)\cdot10^{-6}$
σ_{spec} (200 °C)/S · cm^{-1}	$1.6(3)\cdot10^{-5}$	$3.7(8)\cdot10^{-5}$
σ_{spec} (250 °C)/S · cm^{-1}	$4.7(3)\cdot10^{-5}$	$1.2(2)\cdot10^{-4}$
σ_{spec} (300 °C)/S · cm^{-1}	$1.1(1)\cdot10^{-4}$	$4.5(4)\cdot10^{-4}$
E_a/eV	0.53(1)	0.50(1)

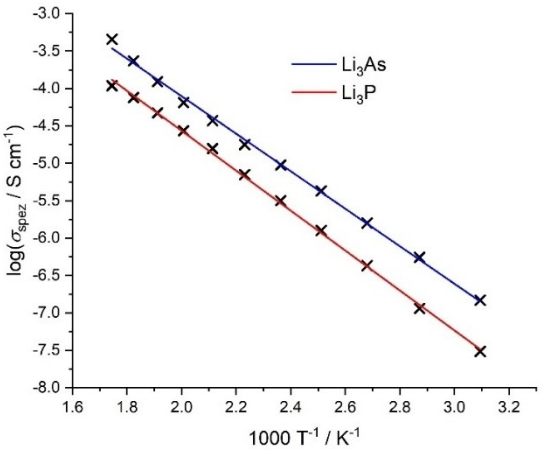

Figure 6. Arrhenius plot of Li_3P and Li_3As from impedance spectra with linear fit showing increasing conductivity with increasing temperature.

Conclusion

We can show that Li_3As is not a metallic compound as proposed by earlier publications.[8] The coloured, hard and brittle samples of Li_3P and Li_3As show increasing conductivity with increasing temperature. The isostructural compounds β-Li_3N, Li_3P and Li_3As crystallizing in the hexagonal [Na_3As]-type structure are obviously lithium-ion conductors. Anyhow, small electronic contributions to total conductivities cannot be excluded. Further measurements are scheduled. The Arrhenius plots for Li_3P and Li_3As show a slightly higher total conductivity and lower activation energy for Li_3As. This is at the significance limit and might be explained by the higher polarizability of the arsenide anion as compared to the phosphide, or due to slightly higher electronic conductivity of the arsenide. This matches the properties of Li_3As calculated by other groups. Temperature dependent powder X-ray diffraction experiments show linear expansion of the unit cell volumes of both compounds with increasing temperature; no hints for phase transitions are observed in the temperature range under investigation. Applying a pressure of about 1.1 GPa for Li_3P and 1.5 GPa for Li_3As, respectively, should lead to a phase transition to the cubic [Li_3Bi]-type structure as shown by DFT calculations. These calculations are in agreement with experimental observations reported in literature. In-situ powder diffraction experiments under high pressure are necessary to confirm this change of the structure. Thermal analyses do not show any effect up to 800 °C. Further experiments are now scheduled to synthesize ternary compounds containing lithium and arsenic to better understand ion conductivity properties in heavy-element frameworks.

Experimental Section

All manipulations were carried out in a Glovebox (MBraun) with oxygen and moisture levels below 0.5 ppm. Synthesis: Li_3P and Li_3As were synthesized from metallic Li (Merck, 99 %) and arsenic (ChemPur, sublimed) or red phosphorus (Hoechst, 99.9 %). Lithium pieces were placed in a graphite container and covered with finely powdered arsenic or phosphorus. A standard batch contains about 500 mg substance. The container was closed with a lid and sealed in a quartz ampoule. Brittle samples of both compounds were obtained by heating the ampoules to 650 °C within 24 h, holding the temperature for 24 h before switching the furnace off. Powder diffraction: The samples were ground in a mortar and filled in a glass capillary (Ø = 0.3 mm). The flame-sealed capillary was mounted on a STOE STADI P diffractometer (Stoe & Cie) equipped with a Mythen 1 K detector for data collection and a graphite furnace for high temperature measurements. Cu$K\alpha_1$ – radiation (λ = 1.540598 Å) was used in all measurements. Raw data was processed with the *WinXPOW* software package (Stoe & Cie), Rietveld refinements were performed with the *Jana2006* program.[21,22] DTA: Samples were ground in Argon atmosphere and prepared in flame-sealed quartz tubes (Ø = 2 mm). Measurements were carried out using a SETARAM TG-DTA 92.16.18 up to 800 °C. Impedance spectroscopy: Impedance measurements to determine the conductivity of the sample were carried out on a Zahner Zennium impedance analyzer coupled with an Eurotherm heating device located in a Glovebox (M Braun) with oxygen and moisture levels below 0.5 ppm. The cold-pressed pelletized sample (Ø = 8 mm) was sandwiched between gold foil and contacted with platinum electrodes. Measurements were carried out from 50 °C up to 300 °C in 25 °C steps in the frequency range from 1 MHz to 100 mHz. Cooling of the inert atmosphere in the glovebox remains difficult, so we cannot provide data at room temperature. The software *Zahner Analysis* was used for raw data processing and fitting.[23] DFT-modelling: calculations were performed in the framework of DFT using the CRYSTAL17 code. Basis sets were taken from literature.[24–25] Structures were fully optimized starting from the structure models obtained from Rietveld-refinements. For all calculations, the PBE-functional with a *k*-mesh sampling of 6×6×6 was used.[26] The convergence criterion was set to 10^{-8} atomic units. Energy vs. volume curves were computed for both models, the obtained data points were fitted to a Birch-Murnaghan EoS.[27,28,29]

Acknowledgements

Open Access funding enabled and organized by Projekt DEAL.

Conflict of Interest

The authors declare no conflict of interest.

Data Availability Statement

The data that support the findings of this study are available on request from the corresponding author. The data are not publicly available due to privacy or ethical restrictions.

Keywords: Li_3As · Li_3P · ion conductivity · impedance spectroscopy · DFT modeling

[1] A. Lazicki, B. Maddox, W. J. Evans, C.-S. Yoo, A. K. McMahan, W. E. Pickett, R. T. Scalettar, M. Y. Hu, P. Chow, *Phys. Rev. Lett.* **2005**, *95*, 165503.
[2] M. E. Leonova, I. K. Bdikin, S. A. Kulinich, O. K. Gulish, L. G. Sevastyanova, K. P. Burdina, *Inorg. Mater.* **2003**, *39*, 266–270.
[3] H. J. Beister, J. Klein, I. Schewe, K. Syassen, *High Pressure Res.* **1991**, *7*, 91–95.
[4] B. A. Boukamp, R. A. Huggins, *Mat. Res. Bull.* **1978**, *13*, 23–32.
[5] U. V. Alpen, A. Rabenau, G. H. Talat, *Appl. Phys. Lett.* **1977**, *30*, 621–623.
[6] H. Yamane, S. Kikkawa, M. Koizumi, *Solid State Ionics* **1987**, *25*, 183–191.
[7] E.-. M. Bertschler, T. Bräuniger, C. Dietrich, J. Janek, W. Schnick, *Angew. Chem. Int. Ed.* **2017**, *56*, 4806–4809; *Angew. Chem.* **2017**, *129*, 4884–4887.
[8] G. A. Nazri, C. Julien, H. S. Mavi, *Solid State Ionics* **1994**, *70/71*, 137–143.
[9] S. Wu, S. N. Neo, Z. Dong, F. Boey, P. Wu, *J. Phys. Chem. C* **2010**, *114*, 16706–16709.
[10] A. Haffner, T. Bräuniger, D. Johrendt, *Angew. Chem. Int. Ed.* **2016**, *55*, 13585–13588; *Angew. Chem.* **2016**, *128*, 13783–13786.
[11] H. Eickhoff, S. Strangmüller, W. Klein, H. Kirchhain, C. Dietrich, W. G. Zeier, L. van Wüllen, T. F. Fässler, *Chem. Mater.* **2018**, *30*, 6440–6448.

[12] S. Strangmüller, H. Eickhoff, G. Raudaschl-Sieber, H. Kirchhain, C. Sedlmeier, L. van Wüllen, H. A. Gasteiger, T. F. Fässler, *Chem. Mater.* **2020**, *32*, 6925–6934.
[13] A. Haffner, A. K. Hatz, I. Moudrakovski, B. V. Lotsch, D. Johrendt, *Angew. Chem.* **2018**, *130*, 6262–6268.
[14] J. Mark, K. Lee, M. A. T. Marple, S. Lee, S. Sen, K. Kovnir, *J. Mater. Chem.* **2020**, *8*, 3322–3332.
[15] S. Pagano, M. Zeuner, S. Hug, W. Schnick, *Eur. J. Inorg. Chem.* **2009**, *12*, 1579–1584.
[16] L. Toffoletti, H. Kirchhain, J. Landesfeind, W. Klein, L. van Wüllen, H. A. Gasteiger, T. F. Fässler, *Chem. Eur. J.* **2016**, *22*, 17635–17645.
[17] R. Juza, K. Langer, K. von Benda, *Angew. Chem. Int. Ed.* **1968**, *10*, 373–384.
[18] K.-J. Range, P. Hafner, *J. Alloys Compd.* **1994**, *216*, 7–10.
[19] H. Eickhoff, C. Dietrich, W. Klein, W. G. Zeier, T. F. Fässler, *Z. Anorg. Allg. Chem.* **2021**, *647*, 28–33.
[20] W. Li, G. Wu, C. M. Araujo, R. H. Schleicher, A. Blomqvist, R. Ahuja, Z. Xiong, Y. Feng, P. Chen, *Energy Environ. Sci.* **2010**, *3*, 1524–1530.
[21] STOE-WinXPOW, *Vol. Version 3.0.2.5*, STOE & Cie GmbH Darmstadt, **2011**.
[22] V. Petricek, M. Dusek, L. Palatinus, *Z. Kristallogr.* **2014**, *229*, 345.
[23] Zahner-Meßtechnik GmbH& Co. KG, *Vol. Version Z.3.03*, Thales-Flink, Kronach.
[24] D. V. Oliveira, M. F. Peintinger, J. Laun, T. Bredow, *J. Comput. Chem.* **2019**, *40*, 2364–2376.
[25] M. Causa, R. Dovesi, C. Roetti, *Phys. Rev. B.* **1991**, *43*, 11937–11943.
[26] J. P. Perdew, K. Burke, M. Ernzerhof, *Phys. Rev. Lett.* **1996**, *77*, 3865.
[27] F. D. Murnaghan, *Am. J. Math.* **1937**, *59*, 235–260.
[28] F. D. Murnaghan, *Proc. Nat. Acad. Sci.* **1944**, *41*, 244–247.
[29] F. Birch, *Phys. Rev.* **1947**, *71*, 809–824.

Manuscript received: November 30, 2021
Revised manuscript received: February 25, 2022
Accepted manuscript online: March 16, 2022

RESEARCH ARTICLE

Li_3As and Li_3P were synthesized from the elements by a high temperature route. The compounds were characterized by impedance spectroscopy, showing unexpected Li-ion conductivity for Li_3As. DFT-calculations prove literature-known phase transformations to a cubic high-pressure modification of Li_3Pn (Pn = N, P, As, Sb, Bi).

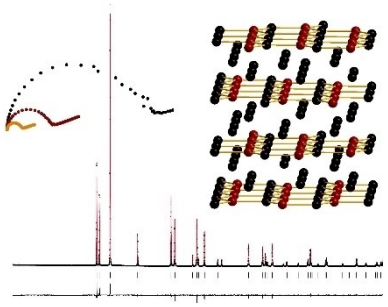

*F. Wegner, F. Kamm, Dr. F. Pielnhofer, Prof. Dr. A. Pfitzner**